NANO LETTERS
Cite This: Nano Lett. 2018, 18, 6057−6063
Letter
pubs.acs.org/NanoLett

New Pathway for Hot Electron Relaxation in Two-Dimensional Heterostructures

Jin Zhang,[†,§,⊥] Hao Hong,[‡] Jia Zhang,[†,⊥] Huixia Fu,[†,⊥] Peiwei You,[†,⊥] Johannes Lischner,[§] Kaihui Liu,[*,‡,#] Efthimios Kaxiras,[*,∥] and Sheng Meng[*,†,⊥,#]

[†]Beijing National Laboratory for Condensed Matter Physics and Institute of Physics, Chinese Academy of Sciences, Beijing 100190, P. R. China

[‡]State Key Laboratory for Mesoscopic Physics, School of Physics, Peking University, Beijing 100871, P. R. China

[§]Departments of Materials and Physics and the Thomas Young Centre for Theory and Simulation of Materials, Imperial College London, London SW7 2AZ, United Kingdom

[∥]Department of Physics and School of Engineering and Applied Sciences, Harvard University, Cambridge, Massachusetts 02138, United States

[⊥]School of Physical Sciences, University of Chinese Academy of Sciences, Beijing 100049, P. R. China

[#]Collaborative Innovation Center of Quantum Matter, Beijing 100190, P. R. China

Supporting Information

ABSTRACT: Two-dimensional (2D) heterostructures composed of transition-metal dichalcogenide atomic layers are the new frontier for novel optoelectronic and photovoltaic device applications. Some key properties that make these materials appealing, yet are not well understood, are ultrafast hole/electron dynamics, interlayer energy transfer and the formation of interlayer hot excitons. Here, we study photoexcited electron/hole dynamics in a representative heterostructure, the MoS_2/WSe_2 interface, which exhibits type II band alignment. Employing time-dependent density functional theory in the time domain, we observe ultrafast charge dynamics with lifetimes of tens to hundreds of femtoseconds. Most importantly, we report the discovery of an interfacial pathway in 2D heterostructures for the relaxation of photoexcited hot electrons through interlayer hopping, which is significantly faster than intralayer relaxation. This finding is of particular importance for understanding many experimentally observed photoinduced processes, including charge and energy transfer at an ultrafast time scale (<1 ps).

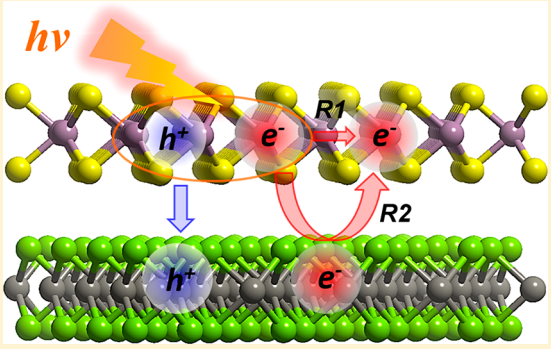

KEYWORDS: *2D heterostructures, van der Waals coupling, ultrafast charge dynamics, hot-electron relaxation, time-domain density functional theory*

Two-dimensional (2D) materials, including graphene and transition-metal dichalcogenides (denoted as MX_2, where M = Mo, W and X = S, Se *etc.*), exhibit intriguing electronic, optical, and mechanical properties, which are significantly different from those of conventional bulk materials.[1−3] The emergence of van der Waals (vdW) heterostructures by stacking different 2D layers vertically paves the way for exploring new interesting physics and device applications.[3−6] Among the heterostructures, those formed by two different monolayers are of particular interest because their electronic and optical properties are tunable. A variety of MX_2 heterostructures have been fabricated and investigated in experiments, including MoS_2/WS_2, $MoS_2/MoSe_2$, and MoS_2/WSe_2.[7−13] In these 2D heterostructures, the reduced dimensionality gives rise to weak screening of electron−electron interactions resulting in large exciton binding energies. Spatial separation of photoexcited electron−hole pairs which is required for efficient conversion of light to electricity or chemical energy is facilitated by type II band alignments.[14−18]

Experimental investigations[19−26] of optical excitation in bilayer MX_2 heterostructures report ultrafast charge dynamics in these systems. For example, Hong et al.[19] observed ultrafast hole transfer from the MoS_2 to the WS_2 layer within ∼50 fs (fs) after photoexcitation. The dependence of interfacial charge dynamics on the bilayer stacking geometry, including translations, rotations and strain, has been studied both experimentally and theoretically.[27−30] Kozawa et al. observed fast interlayer energy transfer (on the order of <1 ps) and showed that energy transfer is the dominant relaxation process in $MoSe_2/WS_2$ bilayers when exciting high-energy electron−

Received: July 23, 2018
Revised: August 9, 2018
Published: August 13, 2018

DOI: 10.1021/acs.nanolett.8b03005
Nano Lett. 2018, 18, 6057−6063

hole pairs in such type II heterostructures.[25] Interestingly, ultrafast interlayer electron transfer in randomly stacked homobilayers such as $MoSe_2/MoSe_2$ and WSe_2/WSe_2 occurs also on a subpicosecond time scale.[26] A detailed understanding of the dynamics of photoexcited carriers is crucial to design and optimize devices as it directly determines the fundamental response speed and photon-electron conversion efficiency. Recent theoretical studies have investigated the mechanisms of charge dynamics in the heterostructures[27−30] but a comprehensive and consistent understanding of the hot electron relaxation processes in MX_2 heterostructures is elusive. Developing further insight requires detailed theoretical investigation to examine different dynamic processes including interlayer charge transfer, energy transfer, and formation of interlayer excitons.

In this work, we investigate the dynamics of photoexcited electron/hole pairs in 2D heterostructures using time-dependent density functional theory in the time domain. Our study reveals significant photoexcited electron and hole transfer from MoS_2 to WSe_2 on a time scale of <100 fs. A detailed analysis of photoinduced electron/hole transfer, energy relaxation and energy transfer explain the differences in interfacial charge dynamics observed in experiments. More importantly, we report the discovery of an interfacial hot-electron relaxation mechanism involving van der Waals interfacial interactions and the assistance of A_{1g} phonons. We compare our results quantitatively to available experimental data. Our results establish a concrete link between the interlayer interactions and electron dynamics in MX_2 heterostructures, providing important insights for future design and optimization of vdW multilayers.

To provide a quantitative description of electron dynamics in the 2D heterostructures using time-domain density functional method, we choose MoS_2/WSe_2 bilayer as a model because it exhibits negligible interlayer strain and ideal type II band alignment.[13,30] The calculations were performed using density functional theory as implemented in the Vienna *ab initio* simulation package[31−33] using the Perdew−Burke−Ernzerhof generalized gradient approximation[34] for the exchange-correlation energy and van der Waals density functional in the opt88 form.[35] We choose the supercells with size of $\sqrt{13} \times \sqrt{13}$ for MoS_2 and $\sqrt{12} \times \sqrt{12}$ for WSe_2, relative to their respective primitive unit cells to minimize the interlayer strain. After geometry optimization at 0 K, the MoS_2/WSe_2 bilayer is heated to 300 K, corresponding to the temperature used in the experiments. After that, 3 ps long adiabatic MD trajectories were generated in the microcanonical ensemble with a 1 fs time step. To simulate the nonadiabatic electron/hole dynamics using fewest switches surface hopping technique,[36−44] 300 geometries were selected randomly from each adiabatic MD trajectory (see Supporting Information for more details).

In Figure 1, we describe the basic physics of electron relaxation processes after photon-induced excitation in a representative system consisting of a MoS_2/WSe_2 bilayer.[11,13] For the case of monolayer MoS_2, optical excitation with high-energy photons (hv > bandgap) results in a photoexcited electron (e^-) - hole (h^+) pair. The energetic or "hot" electron transfers energy to the lattice through electron−phonon interactions and relaxes to the conduction band minimum (CBM), a process we label **R1**. In the MoS_2/WSe_2 bilayer, we find that the hot electron on the MoS_2 layer can also relax through a different process labeled **R2**. In this scenario, the

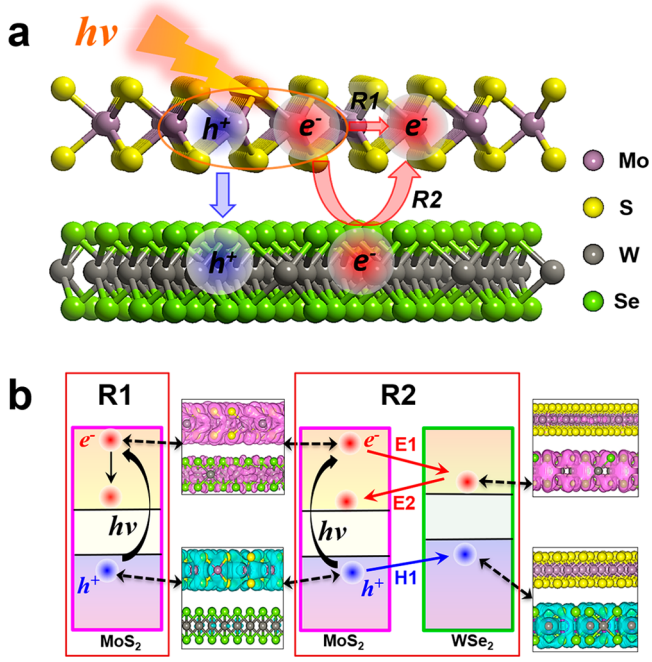

Figure 1. Schematic of the photoinduced carrier dynamics at the MoS_2/WSe_2 interface in real space (a) and energy space (b). **R1**: Conventional relaxation process of hot electron after photoexcitation in MoS_2 monolayer. **R2**: Relaxation process involving interlayer charge transfer. Absorption of a photon by MoS_2 in the heterostructure results in hot-electron (process **E1**) and hole (process **H1**) transfer from MoS_2 to WSe_2 because of the band offsets. After that, the hot electron at WSe_2 transfers back to MoS_2 (process **E2**). The charge distributions (at a contour level of 7×10^{-4} e/Å^3) of the donor and acceptor states are shown in insets, for the electron (in pink) and hole (in light blue). The photoexcited hot electron state (pink) is delocalized between the two layers, indicating a significant interfacial coupling.

interfacial hot-electron transfer first takes place from MoS_2 to WSe_2 (process **E1**) and then the hot electron on the WSe_2 layer moves back to the MoS_2 layer because of its lower CBM (process **E2**), while the photoexcited hole on the MoS_2 layer transfers to the WSe_2 layer (process **H1**). Energy is transferred from MoS_2 to WSe_2 if the hot electron and hole move from MoS_2 to WSe_2 simultaneously. Notably, the competition between the process **R1** in the MoS_2 layer and the alternative (interlayer) charge transfer process **R2** is crucial for designing applications of 2D heterostructures in optoelectronics.

We next discuss in detail the photoexcited carrier dynamics at the MoS_2/WSe_2 interface, as captured by the energy transfer and population decay rates shown in Figure 2. For **R1** (the process of hot-electron relaxation in monolayer MoS_2), we monitor the time evolution of the hot electron state with an initial energy of about ∼1 eV above the CBM of MoS_2. The hot electron loses its excess energy rapidly via electron−phonon and electron−electron interactions. Relaxation to the CBM of MoS_2 takes about 690 fs (via a linear fit to the calculated energy values). In recent ultrafast experiments on MoS_2 monolayers, hot electrons were found to cool down and transfer energy to phonons on a time scale of ∼500 fs after photoexcitation.[10] The agreement between the experimental observations and our simulations confirms the accuracy of our approach (see Supporting Information).

DOI: 10.1021/acs.nanolett.8b03005
Nano Lett. 2018, 18, 6057−6063

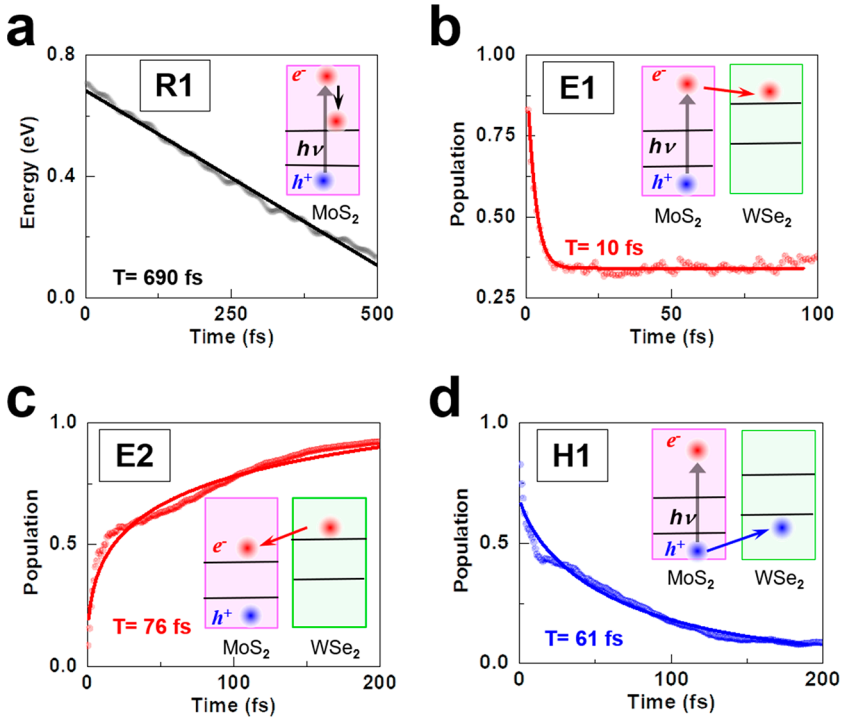

Figure 2. Photoexcitation-induced separate processes at MoS_2/WSe_2 interface. **R1**: Decay of the excitation energy in photoexcited hot-electron relaxation process in single layer MoS_2. The conduction band minimum is set to zero. **E1**: Decay of the population of photoexcited hot electron at MoS_2 due to transfer to WSe_2 on an ultrafast time scale (~10 fs). **E2**: Evolution of population of the hot electron from WSe_2 back to MoS_2. **H1**: Evolution of population of the hole state at MoS_2 being transferred to WSe_2 in an ultrafast time scale (61 fs). The dots in different colors are from our simulations while the solid lines are fitted with exponential functions.

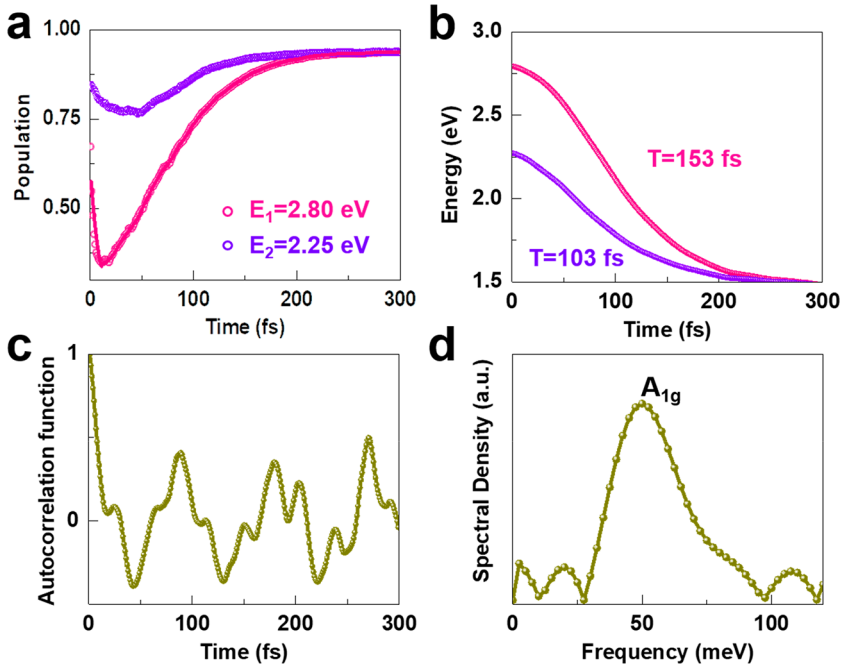

Figure 3. Hot-electron relaxation process at MoS_2/WSe_2 interface. (a) Population at MoS_2 of excited hot electron with initial photoexcited energies of 2.80 eV (in pink) and 2.25 eV (in purple) above the Fermi energy as a function of time after optical absorption. (b) The corresponding energy evolution of excited hot electrons. The hot-electron relaxation pathway, **R2**, corresponds to an ultrafast time scale (~100 fs), which is much faster and more effective than conventional hot-electron relaxation in a single layer (**R1** with time scale ~690 fs). (c) Autocorrelation functions of the photoexcited state (2.80 eV). The similar curve for 2.25 eV is not shown here. (d) Spectral density of the phonon modes during dynamics: A_{1g} is the dominant mode.

For **R2**, we separate the different processes by involving only the relative states with energies in the vicinity of the excited electron/hole state, that is, we switch off surface hopping for states with energies far away from the excited states (see

DOI: 10.1021/acs.nanolett.8b03005
Nano Lett. 2018, 18, 6057−6063

Supporting Information). To analyze the charge transfer dynamics quantitatively, we calculate the probability of finding the electron on a given layer. For the hot electron, the energy of the initial state, after absorbing a high-energy photon, is 1.20 eV above CBM (that is 2.80 eV larger than the Fermi level) of the MoS_2/WSe_2 bilayer and the electron is mostly localized on the MoS_2 layer (~90%). As the state evolves in time, the electron is transferred to the WSe_2 layer. After fitting the electron population on MoS_2 with exponential functions, we find the interfacial hot-electron transfer (process **E1**) takes place on an ultrafast time scale of ~10 fs (the underlying mechanism will be discussed below). In process **E2**, hot electrons are transferred back to the MoS_2 layer. The corresponding charge transfer time from WSe_2 to MoS_2 is about 76 fs, consistent with experimental observation (~40 fs).[20] Meanwhile, the electron transfer to the WSe_2 results in the creation of a hole localized on the MoS_2 layer and photoexcited hole transfers from MoS_2 to WSe_2 in 61 fs (process **H1**), which is attributed to the presence of valence band maximum (VBM) band offset of the bilayer. Our observation that photoexcited electrons and holes on the MoS_2 layer diffuse to the WSe_2 layer on an ultrafast time scale (less than 100 fs) demonstrates that ultrafast energy transfer takes place in the type-II heterostructures.

These findings also explain the ultrafast energy transfer on the order of 1 ps from $MoSe_2$ to WS_2 observed in photoluminescence experiments.[25] As mentioned above, the vertical $MoSe_2/WS_2$ heterostructure has a similar atomic structure as MoS_2/WSe_2 and also features a type-II band offset. Kozawa et al.[25] demonstrated that the energy transfer is Förster-like, that is, photoinduced excitons in the WS_2 layer resonantly produce excitons localized on the $MoSe_2$ layer through dipole−dipole interactions. Thus, energy transfer in vdW heterostructures is highly efficient, despite the type-II band alignment and competing charge transfer, and our results provide insights into the hot-exciton dynamics in MX_2 heterostructures.

We note the multiplication processes (namely, hot electron creates additional excited electrons or holes) may be important in the TMD materials as studies in some recent experiments.[45,46] These processes are very hard to be considered here. This is because our method is based on the hypothesis that the time evolution of a wave packet through a potential-energy region can be regarded as an ensemble of independent semiclassical trajectories. However, the time-domain density functional method is appropriate to reproduce photoexcited phenomena including hot-carrier relaxation because it captures the essential physics, such as detailed balance.[37−39]

To confirm the proposed hot-electron dynamics at the MoS_2/WSe_2 interface, we performed a direct nonadiabatic analysis including all orbitals with energies higher than the CBM of MoS_2. Here, two hot-electron states are selected to analyze the dynamics: one with the energy 2.80 eV and the other with the energy 2.25 eV above the Fermi energy of MoS_2. The results are shown in Figure 3. It is apparent that the hot electron state with the energy 2.80 eV (initially located mostly on the MoS_2 layer) transfers to WSe_2 in less than 10 fs (Figure 3a). The probability of finding the electron on the MoS_2 layer decreases from 75% to 35% during this stage. After that, the hot electron diffuses back to MoS_2 and the population on MoS_2 increases to 93% on a time scale of ~150 fs. The energy of the state decreases continuously from 2.80 to 1.80 eV after photoexcitation (Figure 3b). Fitting to an exponential yields a time scale of 153 fs for this process. Similar dynamics is observed for the hot-electron state with the energy 2.25 eV above the Fermi energy. These results reveal that there exists a robust relaxation process via interlayer hopping on a time scale of ~100 fs. Therefore, we postulate the pathway **R2** is robust and operates in addition to the conventional decay process **R1** at the interfaces, which is consistent with the experimental observation of ultrafast energy dynamics in MX_2 heterostructures. The novel pathway incudes two major steps: the immediate hot electron transfer from MoS_2 to WSe_2 in <10 fs and the subsequent diffusion back from WSe_2 to MoS_2 in ~100 fs. In contrast, the conventional process **R1** operates at a considerably longer time scale, in our simulations ~700 fs.

It has been revealed that defects can effectively modulate the electron−hole recombination after photoexcitation in experiments.[10] Li et al. have found sulfur adatom and vacancy in monolayer MoS_2 can accelerate nonradiative charge carrier recombination using the same first-principle methods.[11] To gain a deep insight in defect effect in hot-carrier relaxation, we performed additional calculations for MoS_2 monolayer with sulfur defects (see Supporting Information). We find sulfur defects can facilitate hot electron relaxation time from ~600 to 200 fs, which is on the same order of magnitude as the pathway predicted (~100 fs). In reality, the 2.8% defect level is quite high, and better control below this defect concentration is needed.[10] Thus, the interfacial hot-electron relaxation should be carefully considered for the heterostructures with defects and trap states in future experiments and applications.

To further understand the pathway for photoexcited hot-electron relaxation, we analyze the effects of phonon vibrations. Vibrational motions promote charge transfer and they are responsible for energy losses to heat. This is because electron−phonon interaction provides crucial channel for hot-electron relaxation.[48−52] We present the normalized energy gap autocorrelation function (ACF) and corresponding Fourier transform (see Supporting Information for details) in Figure 3, parts c and d, respectively. The ACF of the photoexcited state exhibits how the energy at a specific time depends on its previous values. In the heterostructure, the normalized ACF for the state at 2.80 eV decreases rapidly from 1 to 0 within 20 fs. After that, it oscillates significantly with a dominant period of ~90 fs. The oscillation amplitude reaches 40% of the initial value, reflecting that the memory of the energy fluctuation extends into several hundreds of femtoseconds.

Furthermore, Fourier transformation of the energy difference (see Supporting Information for methods) along the molecular dynamics trajectory reveals that the out-of-plane A_{1g} phonon mode (~49.6 meV or ~400 cm^{-1}) in MoS_2/WSe_2 bilayer indeed plays a dominant role in the ultrafast hot-electron dynamics (Figure 3d). For MoS_2, the Raman active S−Mo A_{1g} mode[49−51] has a frequency of ~404 cm^{-1} and the vibrational frequency of A_{1g} mode was reported to be 309 cm^{-1} for WSe_2. In addition, the small peak at 165 cm^{-1} (20.5 meV) may be assigned either to the E^1_g mode of WSe_2 (176 cm^{-1}) or to longitudinal acoustic phonons of MoS_2 at the M point (~226 cm^{-1}).[52−54] The mode at 870 cm^{-1} can be regarded as an overtone of the lower frequencies.

Charge dynamics is more efficient in the presence of electron−phonon coupling. Note that the A_{1g} mode is one of the most prominent Raman modes in TMDs, indicating strong electron−phonon coupling. The strong coupling of A_{1g} phonon modes, involving out-of-plane vibrations of S and Se atoms, is due to the large associated modification of the

DOI: 10.1021/acs.nanolett.8b03005
Nano Lett. 2018, 18, 6057−6063

distance between van der Waals layers. It follows that these modes present a large response to a transverse electric field associated with charge transfer as evidenced by the substantial peaks of the A_{1g} mode in MoS_2 and WSe_2. The out-of-plane displacements of Mo, W, S, and Se have a strong effect on the electron, hole, and energy relaxation dynamics, because these motions modulate the energies of MoS_2 and WSe_2 electronic states and change the donor−acceptor coupling. This can also be attributed to the collective motions modulating the energies of MoS_2 and WSe_2 electronic states and change the donor−acceptor coupling. The E_{1g} mode at around 176 cm^{-1} represents the interlayer sliding mode between MoS_2 and WSe_2 layers, which is relatively less important in the charge dynamics. It is quite intuitive that both MoS_2 and WSe_2 modes participate in electron and hole transfer, because the initially photoexcited states for both processes are delocalized significantly in the heterostructure. Thus, we deduce that the broad peaks (especially the A_{1g} mode) in Figure 3d are attributed to interfacial interactions between MoS_2 and WSe_2 layers. It is not surprising that phonon modes of both MoS_2 and WSe_2 are involved to assist the hot-electron relaxation. This observation, together with strong coupling between MoS_2 and WSe_2 layers, elucidates the mechanism of the novel hot−electron decay channel.

We note that similar processes of hot carrier relaxation have been reported in some recent studies involving chemically bound quantum dots and molecule-semiconductor interfaces.[14−16] Tisdale et al. have found a similar pathway existed in a semiconductor nanocrystal PbSe nanocrystal on bulk TiO_2.[14] Chu et al. have studied the forward and reverse hole transfer between TiO_2 and CH_3OH as well as the hole energy relaxation to the valence band maximum.[15] In addition, experimental works by Chen et al. confirmed ultrafast reverse hole transfer at the interface of the photoexcited methanol/graphitic carbon nitride system. The reverse hole transfer process was found to occur on a time scale of a few hundreds of femtoseconds.[16]

In addition, one may ask whether this hot-electron relaxation process is unique to 2D type II heterostructures. To answer this question, we study the relaxation process in type II core−shell quantum dots (e.g., CdSe/PbSe), which are also widely studied.[45−47] We observed (see Supporting Information for details) that the photoexcited hot electron in CdSe transfers to PbSe in about 10 fs first. Then the hot electron diffuses back to CdSe in about 80 fs, resulting in a similar interfacial hot-electron relaxation pathway. The fundamental distinction of 2D materials lies at the relatively week van der Waals interactions in the component monolayers. In the core−shell quantum dots, the two parts are strongly bonded, resulting in crucial interfacial strains and hybridization of electronic states.

The above findings provide a new view of MX_2 heterostructures for designing potential applications: the novel hot-electron relaxation process facilitated by interfacial interactions should be considered more carefully in promising solar cells or optical detectors. In this regard, one can predict that in vdW-coupled multilayers consisting of different 2D materials, photoexcited hot electrons in one layer will diffuse vertically to other adjacent layers rather than decay thermally within the same layer, as indicated schematically in Figure 4. This leads to a relatively long vertical diffusion channel for hot electrons and minimizes carrier annihilation. The efficient and interlayer-interaction-assisted relaxation channel may also be extended to other types of heterostructures for light-to-electricity conversion, for example, in semiconductor-metal contacts or semiconductor-molecule coupled systems.

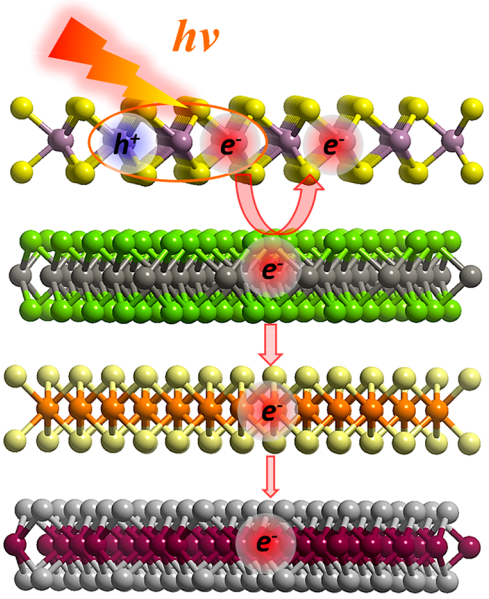

Figure 4. Device concept based on the intriguing relaxation pathway. In the heterostructure with MX_2 layers (different colors represent distinct types of layers), the photoinduced hot electron (e^-) in one layer will diffuse to the adjacent layers (red arrows) vertically following the **R2** relaxation pathway. Here, we suppose the hole state (h^+) is excited to the valence band maximum of the first layer.

In conclusion, *ab initio* time-domain density functional theory simulations reveal a clear and detailed understanding of photoexcited carrier dynamics in the heterostructures comprising MX_2 layers. Our results not only explain well the experimentally observed ultrafast electron/hole dynamics, but also provide insight into the ultrafast energy transfer observed experimentally in heterostructures with type II band alignments. Most importantly, we report that heterostructures bound by vdW interactions can mediate the charge dynamics effectively, leading to a novel pathway for hot electron relaxation through interlayer hopping. The competition between in-plane relaxation processes and interface-assisted interlayer relaxation pathway deserves to be taken carefully into consideration in designing devices based on these heterostructures. Specifically, by manipulating interfacial interactions and fine-tuning the band alignment, it may be possible to control the localization of carriers and the ultrafast dynamics in quantum layered materials.

■ ASSOCIATED CONTENT

Supporting Information

The Supporting Information is available free of charge on the ACS Publications website at DOI: 10.1021/acs.nanolett.8b03005.

Atomic and electronic structures, PDOS of the MoS_2/WSe_2 bilayer, defect effect in hot carrier relaxation in MoS_2 monolayer, hot-electron relaxation process in model core−shell quantum dot, and theoretical methodology (PDF)

DOI: 10.1021/acs.nanolett.8b03005
Nano Lett. 2018, 18, 6057−6063

AUTHOR INFORMATION

Corresponding Authors

*(S.M.) E-mail: smeng@iphy.ac.cn. Telephone: +86 10 82649396.
*(E.K.) E-mail: kaxiras@physics.harvard.edu.
*(K.L.) E-mail: khliu@pku.edu.cn.

ORCID

Jin Zhang: 0000-0001-7830-3464
Kaihui Liu: 0000-0002-8781-2495
Sheng Meng: 0000-0002-1553-1432

Author Contributions

S.M., E.K. and K.L. designed the research. Most of the calculations were performed by J.Z. and H.F. with contributions from all authors. All authors contributed to the analysis and discussion of the data and the writing of the manuscript.

Notes

The authors declare no competing financial interest.

ACKNOWLEDGMENTS

The authors thank Zijing Ding for fruitful discussions. This work was supported by the National Key Research and Development Program of China (Grant Nos. 2016YFA0300902, 2015CB921001 and 2016YFA0300903), the National Natural Science Foundation of China (Grant Nos. 11774396, 11474328 and 51522201), and the "Strategic Priority Research Program (B)" of the Chinese Academy of Sciences (Grant No. XDB07030100). E.K. acknowledges support from ARO MURI Award No. W911NF-14-0247 and STC center for Integrated Quantum Materials, NSF Grant No. DMR-1231319. J.Z. acknowledges funding through the Royal Society Global Challenges Grant CHG\R1\170063.

REFERENCES

(1) Geim, A. K.; Novoselov, K. S. *Nat. Mater.* **2007**, *6*, 183.
(2) Mak, K. F.; Lee, C.; Hone, J.; Shan, J.; Heinz, T. F. *Phys. Rev. Lett.* **2010**, *105*, 136805.
(3) Geim, A. K.; Grigorieva, I. V. *Nature* **2013**, *499*, 419−425.
(4) Yu, W. J.; Liu, Y.; Zhou, H. L.; Yin, A. X.; Li, Z.; Huang, Y.; Duan, X. F. *Nat. Nanotechnol.* **2013**, *8*, 952−958.
(5) Lee, C. H.; Lee, G. H.; van der Zande, A. M.; Chen, W. C.; Li, Y. L.; Han, M. Y.; Cui, X.; Arefe, G.; Nuckolls, C.; Heinz, T. F.; Guo, J.; Hone, J.; Kim, P. *Nat. Nanotechnol.* **2014**, *9*, 676−681.
(6) Rivera, P.; Seyler, K. L.; Yu, H. Y.; Schaibley, J. R.; Yan, J. Q.; Mandrus, D. G.; Yao, W.; Xu, X. D. *Science* **2016**, *351*, 688−691.
(7) Liu, K. H.; Zhang, L. M.; Cao, T.; Jin, C. H.; Qiu, D. A.; Zhou, Q.; Zettl, A.; Yang, P. D.; Louie, S. G.; Wang, F. *Nat. Commun.* **2014**, *5*, 4966.
(8) Gong, Y. J.; Lin, J. H.; Wang, X. L.; Shi, G.; Lei, S. D.; Lin, Z.; Zou, X. L.; Ye, G. L.; Vajtai, R.; Yakobson, B. I.; Terrones, H.; Terrones, M.; Tay, B. K.; Lou, J.; Pantelides, S. T.; Liu, Z.; Zhou, W.; Ajayan, P. M. *Nat. Mater.* **2014**, *13*, 1135−1142.
(9) Fang, H.; Battaglia, C.; Carraro, C.; Nemsak, S.; Ozdol, B.; Kang, J. S.; Bechtel, H. A.; Desai, S. B.; Kronast, F.; Unal, A. A.; et al. *Proc. Natl. Acad. Sci. U. S. A.* **2014**, *111* (17), 6198−6202.
(10) Wang, H.; Zhang, C.; Rana, F. *Nano Lett.* **2015**, *15* (1), 339−345.
(11) Li, L.; Long, R.; Bertolini, T.; Prezhdo, O. V. *Nano Lett.* **2017**, *17*, 7962−7967.
(12) Rivera, P.; Schaibley, J. R.; Jones, A. M.; Ross, J. S.; Wu, S. F.; Aivazian, G.; Klement, P.; Seyler, K.; Clark, G.; Ghimire, N. J.; Yan, J. Q.; Mandrus, D. G.; Yao, W.; Xu, X. D. *Nat. Commun.* **2015**, *6*, 6242.
(13) Chiu, M. H.; Zhang, C. D.; Shiu, H. W.; Chuu, C. P.; Chen, C. H.; Chang, C. Y. S.; Chen, C. H.; Chou, M. Y.; Shih, C. K.; Li, L. J. *Nat. Commun.* **2015**, *6*, 7666.
(14) Tisdale, W. A.; Williams, K. J.; Timp, B. A.; Norris, D. J.; Aydil, E. S.; Zhu, X. Y. *Science* **2010**, *328*, 1543−1547.
(15) Chu, W. B.; Saidi, W. A.; Zheng, Q. J.; Xie, Y.; Lan, Z. G.; Prezhdo, O. V.; Petek, H.; Zhao, J. J. *J. Am. Chem. Soc.* **2016**, *138*, 13740−13749.
(16) Chen, Z.; Zhang, Q.; Luo, Y. *Angew. Chem., Int. Ed.* **2018**, *57*, 5320−5324.
(17) Kim, J.; Bergren, M. R.; Park, J. C.; Adhikari, S.; Lorke, M.; Fraunheim, T.; Choe, D. H.; Kim, B.; Choi, H.; Gregorkiewicz, T.; Lee, Y. H. *arXiv 1801.01675*, 2018.
(18) Barati, F.; Grossnickle, M.; Su, S.; Lake, R. K.; Aji, V.; Gabor, N. M. *Nat. Nanotechnol.* **2017**, *12*, 1134−1139.
(19) Hong, X. P.; Kim, J.; Shi, S. F.; Zhang, Y.; Jin, C. H.; Sun, Y. H.; Tongay, S.; Wu, J. Q.; Zhang, Y. F.; Wang, F. *Nat. Nanotechnol.* **2014**, *9*, 682−686.
(20) Ceballos, F.; Bellus, M. Z.; Chiu, H. Y.; Zhao, H. *ACS Nano* **2014**, *8*, 12717−12724.
(21) Chen, H. L.; Wen, X. W.; Zhang, J.; Wu, T. M.; Gong, Y. J.; Zhang, X.; Yuan, J. T.; Yi, C. Y.; Lou, J.; Ajayan, P. M.; Zhuang, W.; Zhang, G. Y.; Zheng, J. R. *Nat. Commun.* **2016**, *7*, 12512.
(22) Ceballos, F.; Ju, M. G.; Lane, S. D.; Zeng, X. C.; Zhao, H. *Nano Lett.* **2017**, *17*, 1623−1628.
(23) Zhu, H.; Wang, J.; Gong, Z.; Kim, Y. D.; Hone, J.; Zhu, X. Y. *Nano Lett.* **2017**, *17*, 3591−3598.
(24) Zhu, X. Y.; Monahan, N. R.; Gong, Z. Z.; Zhu, H. M.; Williams, K. W.; Nelson, C. A. *J. Am. Chem. Soc.* **2015**, *137*, 14230−14230.
(25) Kozawa, D.; Carvalho, A.; Verzhbitskiy, I.; Giustiniano, F.; Miyauchi, Y.; Mouri, S.; Castro Neto, A. H.; Matsuda, K.; Eda, G. *Nano Lett.* **2016**, *16*, 4087−4093.
(26) Li, Y.; Cui, Q.; Ceballos, F.; Lane, S. D.; Qi, Z.; Zhao, H. *Nano Lett.* **2017**, *17* (11), 6661−6666.
(27) Long, R.; Prezhdo, O. V. *Nano Lett.* **2016**, *16*, 1996−2003.
(28) Wang, H.; Bang, J.; Sun, Y. Y.; Liang, L. B.; West, D.; Meunier, V.; Zhang, S. B. *Nat. Commun.* **2016**, *7*, 11504.
(29) Zhang, J.; Hong, H.; Lian, C.; Ma, W.; Xu, X. Z.; Fu, H. X.; Liu, K. H.; Meng, S. *Adv. Sci.* **2017**, *4*, 1700086.
(30) Ji, Z.; Hong, H.; Zhang, J.; Zhang, Q.; Huang, W.; Cao, T.; Qiao, R.; Liu, C.; Liang, J.; Jin, C.; et al. *ACS Nano* **2017**, *11*, 12020−12026.
(31) Kresse, G.; Furthmüller, J. *Phys. Rev. B: Condens. Matter Mater. Phys.* **1996**, *54*, 11169−11185.
(32) Blöchl, P. E. *Phys. Rev. B: Condens. Matter Mater. Phys.* **1994**, *50*, 17953−17979.
(33) Kresse, G.; Joubert, D. *Phys. Rev. B: Condens. Matter Mater. Phys.* **1999**, *59* (3), 1758.
(34) Perdew, J. P.; Burke, K.; Ernzerhof, M. *Phys. Rev. Lett.* **1996**, *77*, 3865−3868.
(35) Klimeš, J.; Bowler, D. R.; Michaelides, A. *J. Phys.: Condens. Matter* **2010**, *22* (2), 022201.
(36) Tully, J. C. *J. Chem. Phys.* **1990**, *93*, 1061−1071.
(37) Craig, C. F.; Duncan, W. R.; Prezhdo, O. V. *Phys. Rev. Lett.* **2005**, *95*, 163001.
(38) Fischer, S. A.; Habenicht, B. F.; Madrid, A. B.; Duncan, W. R.; Prezhdo, O. V. *J. Chem. Phys.* **2011**, *134*, 024102.
(39) Akimov, A. V.; Prezhdo, O. V. *J. Chem. Theory Comput.* **2013**, *9*, 4959−4972.
(40) Jaeger, H. M.; Fischer, S.; Prezhdo, O. V. *J. Chem. Phys.* **2012**, *137* (22), 22A545.
(41) Madrid, A. B.; Hyeon-Deuk, K.; Habenicht, B. F.; Prezhdo, O. V. *ACS Nano* **2009**, *3*, 2487−2494.
(42) Prezhdo, O. V. *J. Chem. Phys.* **1999**, *111*, 8366−8377.
(43) Long, R.; English, N. J.; Prezhdo, O. V. *J. Am. Chem. Soc.* **2012**, *134*, 14238−14248.
(44) Zheng, Q.; Saidi, W. A.; Xie, Y.; Lan, Z.; Prezhdo, O. V.; Petek, H.; Zhao, J. *Nano Lett.* **2017**, *17* (10), 6435−6442.
(45) Cirloganu, C. M.; Padilha, L. A.; Lin, Q.; Makarov, N. S.; Velizhanin, K. A.; Luo, H.; Robel, I.; Pietryga, J. M.; Klimov, V. I. *Nat. Commun.* **2014**, *5*, 4148.

DOI: 10.1021/acs.nanolett.8b03005
Nano Lett. 2018, 18, 6057−6063

(46) Pietryga, J. M.; Park, Y.-S.; Lim, J.; Fidler, A. F.; Bae, W. K.; Brovelli, S.; Klimov, V. I. *Chem. Rev.* **2016**, *116*, 10513−10622.
(47) Prezhdo, V. *Acc. Chem. Res.* **2009**, *42* (12), 2005−2016.
(48) Huang, S. X.; Liang, L. B.; Ling, X.; Puretzky, A. A.; Geohegan, D. B.; Sumpter, B. G.; Kong, J.; Meunier, V.; Dresselhaus, M. S. *Nano Lett.* **2016**, *16*, 1435−1444.
(49) Zhang, C. D.; Chuu, C. P.; Ren, X. B.; Li, M. Y.; Li, L. J.; Jin, C. H.; Chou, M. Y.; Shih, C. K. *Sci. Adv.* **2017**, *3*, e1601459.
(50) Chiu, M. H.; Li, M.Y.; Zhang, W.; Hsu, W. T.; Chang, W. H.; Terrones, M.; Terrones, H.; Li, L. J. *ACS Nano* **2014**, *8* (9), 9649−9656.
(51) Berkdemir, A.; Gutiérrez, H. R.; Botello-Méndez, A. R.; Perea-López, N.; Elías, A. L.; Chia, C. I.; Wang, B.; Crespi, V. H.; López-Urías, F.; Charlier, J. C.; et al. *Sci. Rep.* **2013**, *3*, 1755.
(52) Lee, C.; Yan, H.; Brus, L. E.; Heinz, T. F.; Hone, J.; Ryu, S. *ACS Nano* **2010**, *4*, 2695−2700.
(53) Li, H.; Zhang, Q.; Yap, C. C. R.; Tay, B. K.; Edwin, T. H. T.; Olivier, A.; Baillargeat, D. *Adv. Funct. Mater.* **2012**, *22* (7), 1385−1390.
(54) Luo, X.; Zhao, Y.; Zhang, J.; Toh, M.; Kloc, C.; Xiong, Q.; Quek, S. Y.; et al. *Phys. Rev. B: Condens. Matter Mater. Phys.* **2013**, *88* (19), 195313.

DOI: 10.1021/acs.nanolett.8b03005
Nano Lett. 2018, 18, 6057−6063